Liquid Crystals
Publication details, including instructions for authors and subscription information:
http://www.informaworld.com/smpp/title~content=t713926090

Analysis of the vibrational spectra of chiral liquid crystalline thioesters

R. Korlacki[ab]; K. Merkel[a]; J. K. Vij[a]; R. Wrzalik[b]; A. Kocot[b]; M. D. Ossowska-Chruściel[c]; J. Chruściel[c]; S. Zalewski[c]
[a] Department of Electronic and Electrical Engineering, Trinity College, University of Dublin, Dublin 2, Ireland [b] Institute of Physics, University of Silesia, 40-007 Katowice, Poland [c] Institute of Chemistry, University of Podlasie, 08-110 Siedlce, Poland

To cite this Article Korlacki, R. , Merkel, K. , Vij, J. K. , Wrzalik, R. , Kocot, A. , Ossowska-Chruściel, M. D. , Chruściel, J. and Zalewski, S.(2006) 'Analysis of the vibrational spectra of chiral liquid crystalline thioesters', Liquid Crystals, 33: 2, 219 — 225
To link to this Article: DOI: 10.1080/02678290500231570
URL: http://dx.doi.org/10.1080/02678290500231570

Liquid Crystals, Vol. 33, No. 2, February 2006, 219–225

Analysis of the vibrational spectra of chiral liquid crystalline thioesters

R. KORLACKI†‡, K. MERKEL†, J.K. VIJ*†, R. WRZALIK‡, A. KOCOT‡, M.D. OSSOWSKA-CHRUŚCIEL§, J. CHRUŚCIEL§ and S. ZALEWSKI§

†Department of Electronic and Electrical Engineering, Trinity College, University of Dublin, Dublin 2, Ireland
‡Institute of Physics, University of Silesia, 40-007 Katowice, Poland
§Institute of Chemistry, University of Podlasie, 08-110 Siedlce, Poland

(*Received 20 January 2005; accepted 7 April 2005*)

Vibrational spectra of (*S*)-(+)-4-(1-methylheptyloxy)biphenyl 4-pentylphenylthiobenzoate (MHOBS5) were calculated using the density functional theory method, with two different basis sets, the 6-31G* and the 6-31+G*. The force fields were scaled using the scaled quantum-mechanical force field (SQM) procedure. Various sets of scaling factors for the SQM procedure are discussed. Results of simulations were used to analyse the experimental data obtained from infrared and Raman experiments for MHOBS5 and the homologous MHOBS4.

1. Introduction

Infrared spectroscopy has been found to be a very powerful technique for investigating the orientational order of liquid crystals [1–9]. Liquid crystalline molecules usually contain more than 50 atoms and the compounds exhibit rather rich spectra. A comparison of the experimental data with the results of the *ab initio* or density functional theory (DFT) calculations lead us to obtaining more complete and reliable information about the molecular system [10–13]. In this paper we show an application of the scaled quantum mechanical (SQM) procedure [14, 15] and its further optimizations [16, 17] for the calculated frequencies of a ferroelectric liquid crystalline thioester. Such a procedure has already been successfully applied to several liquid crystalline systems [18, 19]. The compound under study, (*S*)-(+)-4-(1-methylheptyloxy)biphenyl 4-pentylphenylthiobenzoate, referred to using the acronym MHOBS5, has the molecular structure shown in figure 1, and was synthesized in the University of Podlasie in Siedlce, Poland. MHOBS5 belongs to a new homologous series of chiral thiobenzoates, referred to as (*S*)MHOBS*n*. Recently, a convenient synthesis and the ferroelectric properties of the (*S*)(+)-4-(1-methylheptyloxy)biphenyl 4-alkylthiobenzoates were described [20]. The (*S*)MHOBS*n* series possesses a rich phase polymorphism, including chiral ferroelectric smectic C (SmC*) and cholesteric (N*) phases, as well as two highly ordered tilted phases CrG* and HexI*. A direct transition from N* to SmC* results in a characteristic electro-optic response known as 'half V-shaped switching' [21, 22]. The presence of only one sulphur atom, close to the central part of the molecule, provides the opportunity for carrying out resonant X-ray scattering studies [23]. These facts make the members of the MHOBS*n* series very attractive materials from the scientific, as well as the application points of view. Moreover, their structure makes them very convenient candidates for spectroscopic investigations: the compounds possess only single groups such as the carbonyl group C=O, –C–O–C– and –C–S–C–, which can be seen separately in the vibrational spectra.

For drawing a comparison, the homologous compound MHOBS4, (*S*)-(+)-4-(1-methylheptyloxy)biphenyl 4-butylphenylthiobenzoate, with the non-chiral chain shorter by one CH_2 group, was also studied. The experimental spectra of both compounds were found to be almost exactly the same (see §3.). Therefore, all our considerations are focused on MHOBS5, but it is likely that this may also be very useful for the other homologue and similar compounds.

2. Calculations

All DFT calculations were performed using the Gaussian 98W application [24] running on a personal computer, equipped with 2GB of operational memory. The molecular structure, the harmonic vibrational force constants, and the absolute IR and Raman intensities

*Corresponding author. Email: jvij@tcd.ie

Liquid Crystals
ISSN 0267-8292 print/ISSN 1366-5855 online © 2006 Taylor & Francis
http://www.tandf.co.uk/journals
DOI: 10.1080/02678290500231570

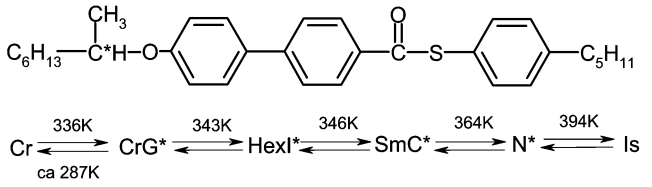

Figure 1. Molecular structure and phase sequence of MHOBS5.

were calculated using the density functional theory, with the hybrid B3LYP functional (Becke's three parameter exchange functional [25] in combination with the Lee–Yang–Parr correlation functional [26]) and two basis sets: the polarized 6-31G* and the diffusive 6-31+G*. B3LYP functional with 6-31G* basis set is commonly used and this method together with the scaling procedures gives very accurate theoretical reproduction of the vibrational spectra. The set 6-31+G*, which differs from the 6-31G* by possessing additional diffusive function on heavy atoms, covers a substantially larger space, and allows better approximation of atomic interactions. The calculation using the diffusive 6-31+G* basis set is much more time consuming, but is recommended for systems with sufficient negative charge (for example, atoms with a free pair of electrons) [27]. The geometry of the investigated structure was initially optimized with a semiempirical AM1 algorithm and then with the quoted DFT method. Next, the optimized geometries were used to obtain vibrational frequencies.

All computational methods show systematic errors in calculating vibrational frequencies, due to the limited range of interactions between a finite number of atoms, basis sets and many different approximations, especially the harmonic approximation. Therefore, the application of a scaling procedure may compensate for these errors. Because the errors are different for different types of force constants, a scaling with a set of several scaling factors is carried out using the equation [14, 15]:

$$F'_{ij} = (\lambda_i \lambda_j)^{1/2} F_{ij} \quad (1)$$

where F'_{ij} is the scaled force constant for the internal coordinates i and j, F_{ij} is the original force constant, and λ_i and λ_j are scaling factors for internal coordinates i and j, respectively, giving the best accuracy. The standard set of scaling factors for the scaled quantum mechanical (SQM) procedure and its further improvements are given in table 1.

3. Experiments

The experiments were performed with a Bio-Rad FTS-6000 Fourier Transform Infrared Spectrometer. The samples were sandwiched between two ZnSe windows, transparent to infrared radiation; the sample thickness was 6 μm. Spectra were collected in the range 3 500–550 cm^{-1}, with a resolution 1 cm^{-1} and an accumulation over 32 scans.

Polarized Raman spectra were recorded using a LabRam multichannel spectrometer comprising an Olympus BX40 confocal microscope. The spectrometer was equipped with a CCD detection system having 1 024 pixels along the dispersion axis and a grating with a groove density of 1 800 per mm. The spectra were collected in the range 50–3 600 cm^{-1} with spectral resolution of 2.8 cm^{-1} and with a data sampling interval of 1 cm^{-1}. An air-cooled argon laser operating at 514.5 nm (JDS Uniphase) with approximately 30 mW of radiation power at the sample was used for excitation. A notch filter was set in the optical path to enhance the rejection of the exciting radiation (this limits the spectrum to Raman shifts over 50 cm^{-1}). Generally, the spectra were recorded ten times with an accumulation time of 30 s. The spectral frequencies were calibrated with the Si line and are accurate to $\pm 0.5\,cm^{-1}$. The

Table 1. Scaling factors for the SQM procedure. X, Y, Z denote heavy atoms.

Symmetry of modes	Standard factor [15]	Refined factor	Ref.
X–Y stretching	0.922	0.9254	[16]
X–H stretching	0.920	0.9182	[16]
X–H stretching (aliph.)		0.889	[17]
X–H stretching (arom.)		0.915	[17]
X–Y–Z bending	0.990	0.9923	[16]
X–Y–H bending	0.950	0.9473	[16]
H–X–H bending	0.915	0.9171	[16]
Out-of-plane	0.976	0.9711	[16]
NH_2 wagging	0.806	0.8358	[16]
X–O–H, X–N–H bending	0.876	0.9047	[16]
Torsions of conjugated systems	0.935	0.9389	[16]
Torsions of single-bonded systems	0.831	0.8980	[16]
Linear deformations	0.913	0.8905	[16]

measurements were made for the crystalline phase (at room temperature) and for the isotropic phase at 400 K.

Figure 2 shows the infrared spectra of the two compounds, MHOBS5 and MHOBS4, in the isotropic phase. This phase was chosen in order to neglect effects due to ordering. Anisotropy may lead to an inadequate comparison of the peak intensities, and therefore all the further analysis, unless otherwise stated, refers to the isotropic phase. There are no significant differences between the spectra of the two compounds. For MHOBS5, an additional experiment was carried out in the SmC* phase. For a very well aligned sample the infrared spectra were collected using the polarized IR beam in directions parallel and perpendicular to the optical axis.

4. Results and discussion

Theoretical spectra obtained with both basis sets were scaled using the standard SQM procedure with three different sets of scaling factors: standard old [15], reoptimized [16] and reoptimized with the scaling factor for the CH stretching vibration divided into two, for hydrogens bonded to aromatic and aliphatic carbons [17]. To compare experimental and theoretical spectra, the gaussian function of the width of 7 cm^{-1}, was replaced on each calculated frequency. Agreement between the experimental spectra and those calculated was checked by drawing a comparison of frequencies of the 33 strongest and well identifiable peaks in all the spectra. Table 2 contains the average deviations of these frequencies.

Looking only at the fingerprint region (2000–500 cm^{-1}), the average deviation changes from *c.* 10 cm^{-1} for the 6-31G* basis set to 8 cm^{-1} for the 6-31+G* set. The most important difference concerns

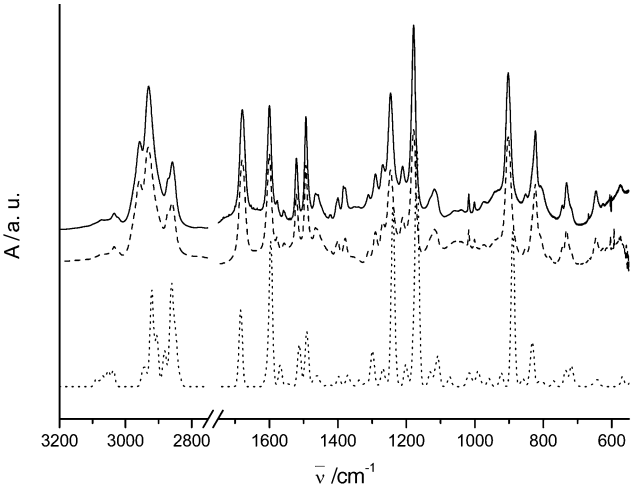

Figure 2. Infrared spectra of MHOBS5 (solid line) and MHOBS4 (dashed line) in the isotropic phase. The dotted line is the calculated spectrum of MHOBS5.

Table 2. Comparison of results obtained with various sets of scaling factors.

Basis set	Set of scaling factors	Average deviation/ cm^{-1}
6-31G*	Standard old	25.1
	Refined by [16]	24.7
	Refined by [16, 17]	13.6
6-31+G*	Standard old	20.8
	Refined by [16]	19.2
	Refined by [16, 17]	8.17

the stretching vibration of the carbonyl bond. It can be seen in the experimental spectrum at 1679 cm^{-1}, while obtained with the polarized basis set (after scaling with the refined set of scaling factors) at 1720 cm^{-1}. The diffusive basis gives reliable value of 1684 cm^{-1}. As mentioned above, the diffusive basis set is recommended for systems with free electrons. In this case, the electronic structure of a close neighbourhood of the oxygen and sulphur can be properly solved only with the diffusive basis.

The range above 2800 cm^{-1}, with the CH stretching modes, is especially difficult to restore. It is caused by anharmonicity, due to a large difference in mass between the hydrogen and the heavy atoms, and perturbed by the Fermi resonance effect. Using scale factors from [17] as well as the diffusive basis, accuracy in this wave number range can be increased (figure 3). Moreover, this significant progress in restoring this region is obtained by applying the diffusive basis on heavy atoms only.

Table 3 gives a detailed list of the experimental spectral bands, along with their assignments based on

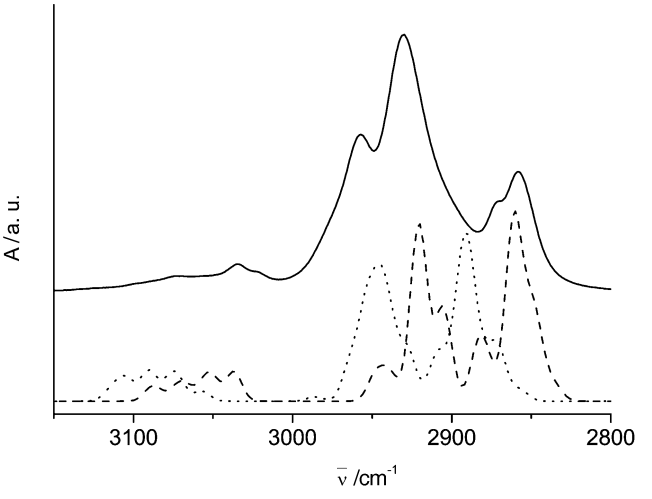

Figure 3. Infrared spectra in the range 3200–2800 cm^{-1} for MHOBS5. The solid line denotes the experimental spectrum (isotropic phase); the dotted line denotes the spectrum calculated with the 6-31G* basis set; the dashed line denotes the spectrum calculated with the 6-31+G* basis set.

Table 3. Vibrational frequencies, and infrared and Raman intensities and their assignments.

Experimental frequency (intensity)[a]		Calculated frequency	
IR	Raman	(IR, Raman intensities)[b]	Assignment (TED %))[c]
—	403 w	401 (0.0, 0.01)	100 τCC (16a)
—	415 vw	412 (0.01,0.02)	70 τCC
		413 (0, 0.04)	34 τCC (16a)
576 vw	575 vw	569 (0.06, 0.02)	19βCCC+11 C_s–S
646 vw	638 vw	642 (0.03, 0)	44 γC−C_s−S=O
721 vw	725 vw	719 (0.04, 0)	71 γCH+15 βCCC (4)
		719 (0.05, 0.01)	39 $\beta_{as}CH_2$
732 w	735 vw	734 (0.08, 0.02)	41 β_{as} CH_2
745 vw	747 vw	738 (0.02, 0)	58 τCC+19 γCC (4)
—	791 vw	770 (0.03, 0.01)	40 $\beta_{as}CH_2$
805 vw	809 vw	812 (0.03, 0)	87 γCH (10a)
823 m	823 vw	830 (0.13, 0.01)	84 γCH (17b)
		834 (0.12, 0)	72 γCH (17b)
852 vw	—	859 (0.03, 0.01)	37 γCH (17b)
902 s	904 vw	889 (0.88, 0.02)	28 δC−C_s–O+18 νCC
938 vw	—	923 (0.08, 0)	33 $\delta_{as}CH_3$+20 νC*–O
974 vw	—	958 (0.04, 0)	48 $\gamma_{as}CH_2$
1001 vw	—	991 (0.08, 0)	47 νC−C
1017 vw	1019 vw	1017 (0.03, 0)	59 βCCC+20 νCC (12)
		1020 (0.04, 0)	30 νCC(18a)
—	1098 vw	1074 (0.0, 0.01)	48 νCC+15 νC−S (18a)
1117 vw	1120 vw	1108 (0.13, 0.01)	22βCCH+19$\delta_{as}CH_3$+16νCC (18b)
1131 vw	—	1131 (0.08, 0)	16 βCH_3+{7 νC*−O}
1179 vs	1182 w	1166 (0.44, 0.14)	23 $\beta_{as}CH_2$
	1187 m	1170 (0.99, 0.28)	34 βCCH+31 νCC (9a)
1210 w	1209 vw	1202 (0.11, 0.01)	40 νCC+26 βCCH (9a)
1246 s	1249 vw	1239 (1.0, 0.03)	38 νC−O+23 νCC
1290 vw	1290 w	1269 (0.10, 0)	49 νCC+16 βCCC (14)
	1299 sh	1276 (0.01, 0.26)	37 νCC+14 βCCC (14)
		1299 (0.18, 0.02)	71 $\gamma_{as}CH_2$
1324 vw	1324 vw	1338 (0.04, 0.01)	40 $\gamma_s CH_2$+40 δC*−H
1378 vw	—	1370 (0.05, 0)	86 $\delta_s CH_3$
1399 vw	1403 vw	1397 (0.05, 0.01)	48 νCC+20 βCC
—	1438 vw	1451 (0.01, 0)	80 $\delta_s CH_3$
1462 w	—	1458 (0.02, 0)	91 $\delta_{as}CH_3$
		1460 (0.01, 0)	84 $\delta_{as}CH_3$
		1460 (0.02, 0)	89 $\delta_{as}CH_3$
		1470 (0.04, 0)	71 $\beta_s CH_2$+24 $\delta_{as}CH_3$
1493 m	1493 vw	1491 (0.28, 0.01)	62 βCCH+12 νCC (19a)
1521 w	1524 vw	1512 (0.23, 0.02)	48 βCCH+26 νCC (19a)
1556 vw	1561 vw	1545 (0.01, 0.01)	55 νCC (8b)
1577 vw	—	1568 (0.12, 0.04)	55 νCC (8b)
1600 m	1601 vs	1596 (0.72, 1.0)	40 νCC (8a)
1679 m	1680 vw	1684 (0.43, 0.08)	90 νC=O
2857 w	2850 vw	2860 (0.5, 0.05)[d]	96–87 $\nu_s CH_2$
2873 w	2873 vw	2882 (0.2, 0.02)[d]	97–95 $\nu_s CH_3$
2931 s	2889 vw	2920 (0.5, 0.02)[d]	95–77 $\nu_{as}CH_2$
	2909 vw		
	2931 vw		
2958 m	2958 vw	2943 (0.1, 0.01)[d]	99–90 $\nu_{as}CH_3$

[a] Key: vw (very weak) 0–20%, w (weak) 20–40%, m (medium) 40–60%, s (strong) 60–80%, vs (very strong) 80–100% with respect to the strongest peak in the spectrum; sh=shoulder. [b] ν=stretching, δ=bending, β=in-plane deformation, γ=out-of-plane deformation, τ=torsion, *s*=symmetric, *as*=asymmetric; C_{ph}, CC, CCC, CCH=aromatic ring; CH_2, CH_3, C−C=alkyl chain, C=O, C−O=ester group, C*=chiral carbon atom, C_s=carbon atom in thioester group. [c] Assignment done using total energy distribution (TED) [33]. Wilson's symbols [34, 35] for principal benzene bands are given in parentheses. [d] Position and intensity for the strongest band, estimated from theoretical spectra.

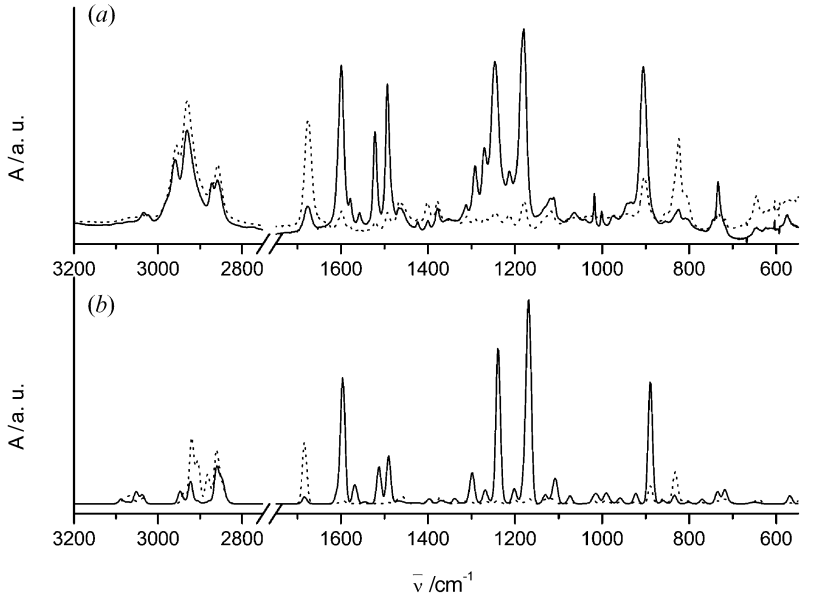

Figure 4. Polarized infrared spectra of MHOBS5: (*a*) experimental spectra in SmC* phase; (*b*) calculated spectra, solid and dotted lines denote polarizations parallel and perpendicular to the optical axis, respectively.

the theoretical spectrum showing the best agreement with experiment (see theoretical spectra in figure 2). For the calculated transition dipole moments the polarized spectra were prepared with directions parallel and perpendicular to the long molecular axis, the latter being defined as the axis of the lowest moment of inertia. Although various other definitions could be considered (for example by the main axes of the polarizability tensor), differences between them are not practically significant [28]. Polarized theoretical spectra are compared with the experimental spectra of the smectic C* phase in figure 4. It is clear, that the optical axis of the sample and the axis of the lowest moment of inertia of the molecule are close; therefore the calculated transition dipole moments may be potentially useful for further orientational studies and especially for a determination of the orientational order parameters [2, 12, 13]. The angles β and φ of transition dipole moments for a few selected infrared bands in the reference system of the moment of inertia are given in table 4. The selected bands were chosen from the most important, non-mixed bands, defined either by a single normal mode or where one mode dominates. The angles are defined as in figure 5.

Figure 6 shows a comparison between the calculated and the experimental Raman spectra in VV and VH geometries. Raman intensities were calculated for backward scattering geometry. The differential Raman scattering cross section of the j-th normal mode was obtained from the absolute Raman activity S_j, given in the output of the Gaussian application by the equation [29]:

$$\frac{\mathrm{d}\sigma_j}{\mathrm{d}\Omega} \approx \frac{(v_0 - v_j)^4}{v_j} \frac{S_j}{1 - \exp\left(-\frac{hcv_j}{kT}\right)} \qquad (2)$$

where v_0 and v_j are the frequencies of the excitation line and the normal mode, respectively; h, c and k are

Table 4. Angles of the calculated transition dipole moments for the selected infrared bands.

Calculated IR freq/ cm^{-1}	Angles of transition dipole moment	
	β/deg	φ/deg
569	18.4	12.5
642	68.6	128
734	24.0	146
770	25.6	137
812	89.7	94.0
889	20.8	145
923	25.6	31.5
991	29.2	41.2
1131	34.7	12.5
1202	29.0	157
1239	9.02	36.5
1269	23.1	18.4
1370	57.6	71.8
1397	35.0	152
1491	9.08	18.9
1512	6.56	58.0
1568	4.77	175
1596	8.86	21.9
1684	71.7	18.4

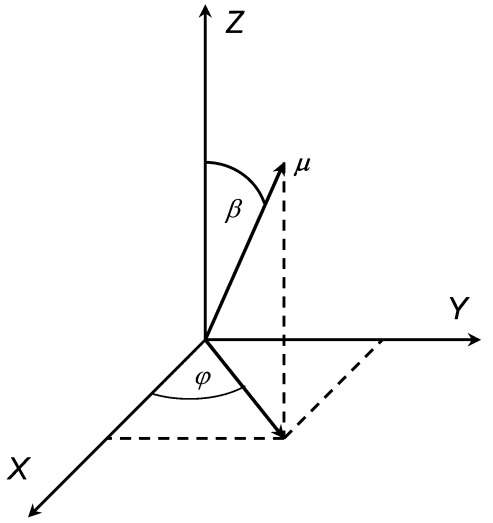

Figure 5. Transition dipole moment μ in the reference system of the moment of inertia; X and Z are axes of the highest and lowest moments of inertia, respectively.

universal constants. The temperature T was chosen to be 400 K.

The presence of the band at 415 cm^{-1} should be particularly noted. This indicates that the phenyl rings in the biphenyl group are twisted with respect to each other. This band has already been used to detect the twisted form of the biphenyl group in several systems including liquid crystals [30–32].

5. Conclusions

The vibrational spectra of a ferroelectric liquid crystal were obtained with an accuracy on average better than 10 cm^{-1}. Application of the DFT theory with the SQM procedure makes it possible to assign the absorption bands and to obtain detailed information about the transition dipole moments, including their orientation and value. We obtained excellent agreement between the calculated and experimental spectra using the diffusive basis set, and by using the same set of scaling factors introduced for the polarized basis. We can also conclude, that a splitting of the scaling factor for CH stretching into parts for hydrogens connected to the aliphatic and the aromatic carbons gives much better accuracy. Such an approach may be recommended particularly for systems such as liquid crystals, which contain long aliphatic chains and several aromatic rings.

Acknowledgments

The authors would like to thank Prof. P. Pulay for his program for SQM calculations. R.K. thanks Dr J. Baker for fruitful discussions. This work was partly supported by The Committee for Scientific Research (KBN) under Grant No. 2P03B 07025. The R.K. predoctoral appointment at Trinity College Dublin is funded by the EU Sampa project (HPRN-CT-2002-00202). Laboratory facilities in Dublin are funded by SFI (02/IN.1/I031).

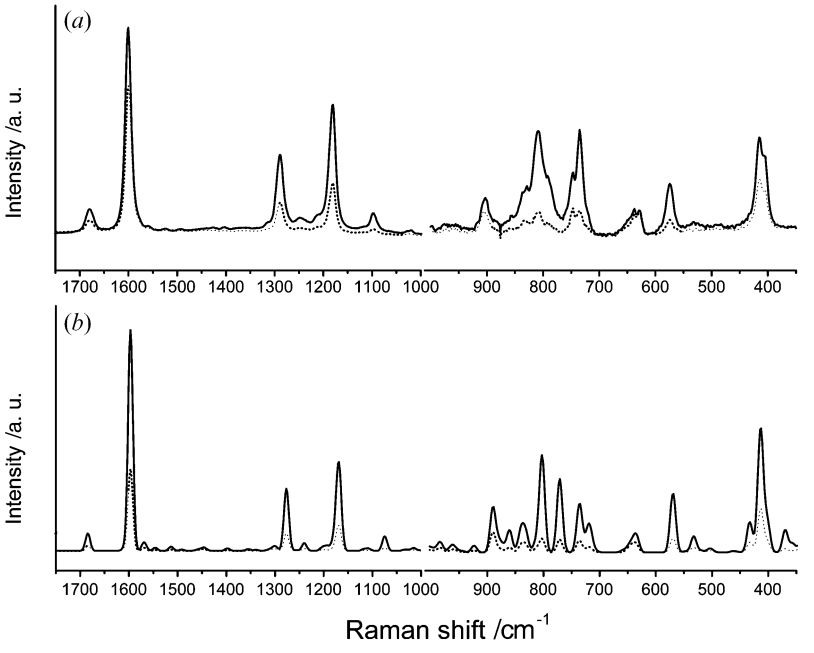

Figure 6. Polarized Raman spectra of MHOBS5: (*a*) experimental spectra in the isotropic phase; (*b*) calculated spectra, solid and dotted lines denote polarized and depolarized spectra, respectively (the region below 1000 cm^{-1} was multiplied by factor 10 due to weakness of the peaks).

K.M. postdoctoral fellowship was funded by the EU LCDD network project (HPRN-CT-2000-00014).

References

[1] A. Kocot, G. Kruk, R. Wrzalik, J.K. Vij. *Liq. Cryst.*, **12**, 1005 (1992).
[2] E. Hild, A. Kocot, J.K. Vij, R. Zentel. *Liq. Cryst.*, **16**, 783 (1994).
[3] K.H. Kim, K. Ishikawa, H. Takezoe, A. Fukuda. *Phys. Rev. E*, **51**, 2166 (1995).
[4] K. Miyachi, J. Matsushima, Y. Takanishi, K. Ishikawa, H. Takezoe, A. Fukuda. *Phys. Rev. E*, **52**, R2153 (1995).
[5] F. Hide, N.A. Clark, K. Nito, A. Yasuda, D.M. Walba. *Phys. Rev. Lett.*, **75**, 2344 (1995).
[6] W.G. Jang, C.S. Park, J.E. Maclennan, K.H. Kim, N.A. Clark. *Ferroelectrics*, **180**, 213 (1996).
[7] A. Kocot, R. Wrzalik, J.K. Vij. *Liq. Cryst.*, **21**, 147 (1996).
[8] S.V. Shilov, H. Skupin, F. Kremer, T. Wittig, R. Zentel. *Phys. Rev. Lett.*, **79**, 1686 (1997).
[9] A. Kocot, R. Wrzalik, B. Orgasinska, T. Perova, J.K. Vij, H.T. Nguyen. *Phys. Rev. E*, **59**, 551 (1999).
[10] R. Wrzalik, K. Merkel, A. Kocot, B. Ciepłak. *J. Chem. Phys.*, **117**, 4889 (2002).
[11] J. Matsushima, Y. Takanishi, K. Ishikawa, H. Takezoe, A. Fukuda, C.S. Park, W.G. Jang, K.H. Kim, J.E. Maclennan, M.A. Glaser, N.A. Clark, K. Takahashi. *Liq. Cryst.*, **29**, 27 (2002).
[12] M.D. Ossowska-Chruściel, R. Korlacki, A. Kocot, R. Wrzalik, J. Chruściel, S. Zalewski. *Phys. Rev. E*, **70**, 41705 (2004).
[13] K. Merkel, A. Kocot, J.K. Vij, R. Korlacki, G.H. Mehl, T. Meyer. *Phys. Rev. Lett.*, **93**, 237801 (2004).
[14] P. Pulay, G. Fogarasi, G. Pongor, J.E. Boggs, A. Vargha. *J. Am. chem. Soc.*, **105**, 7037 (1983).
[15] G. Rauhut, P. Pulay. *J. Phys. Chem.*, **99**, 3093 (1995).
[16] J. Baker, A.A. Jarzecki, P. Pulay. *J. Phys. Chem. A*, **102**, 1412 (1998).
[17] S.A. Katsyuba, J. Grunenberg, R. Schmutzler. *J. Mol. Struct.*, **559**, 315 (2001).
[18] K. Merkel, A. Kocot, R. Wrzalik, B. Orgasińska. *Acta Phys. Polonica A*, **98**, 525 (2000).
[19] K. Merkel, R. Wrzalik, A. Kocot. *J. Mol. Struct.*, **563–564**, 477 (2001).
[20] M.D. Ossowska-Chruściel. *Liq. Cryst.*, **31**, 1159 (2004).
[21] T. Hatano, K. Yamamoto, H. Takezoe, A. Fukuda. *Jpn. J. Appl. Phys. Part 1*, **25**, 1762 (1986).
[22] Y. Asao, T. Togano, M. Terada, T. Moriyama, S. Nakamura, J. Iba. *Jpn. J. Appl. Phys. 1*, **38**, 5977 (1999).
[23] L.S. Hirst, S.J. Watson, H.F. Gleeson, P. Cluzeau, P. Barois, R. Pindak, J. Pitney, A. Cady, P.M. Johnson, C.C. Huang, A.-M. Levelut, G. Srajer, J. Pollmann, W. Caliebe, A. Seed, M.R. Herbert, J.W. Goodby, M. Hird. *Phys. Rev. E*, **65**, 41705 (2002).
[24] M.J. Frisch, et al. Gaussian 98 (Revision A.7), Gaussian Inc., Pittsburgh PA (1998).
[25] A.D. Becke. *J. Chem. Phys.*, **98**, 1372 (1993).
[26] C. Lee, W. Yang, R.G. Parr. *Phys. Rev. B*, **41**, 785 (1988).
[27] J.B. Foresman, A. Frisch, *Exploring Chemistry with Electronic Structure Methods* Gaussian Inc., Pittsburgh and references therein 1996.
[28] M.R. Wilson. *J. Mol. Liq.*, **68**, 23 (1996).
[29] P.L. Polavarapu. *J. Phys. Chem.*, **94**, 8106 (1990).
[30] K. Tashiro, J. Hou, M. Kobayashi, T. Inoue. *J. Am. Chem. Soc.*, **112**, 8273 (1990).
[31] K.H. Kim, Y. Takanishi, K. Ishikawa, H. Takezoe, A. Fukuda. *Liq. Cryst.*, **16**, 185 (1994).
[32] A.E. Keating, S.H. Shin, F.K. Huang, R.L. Garrell, M.A. Garcia-Garibay. *Tetrahedron Lett.*, **40**, 261 (1999).
[33] P. Pulay, E. Török. *Acta Chim. Acad. Sci. Hung.*, **47**, 273 (1966).
[34] E.B. Wilson, J.C. Decius, P.C. Cross. *Molecular Vibrations*. McGraw-Hill, New York (1995).
[35] G. Varsányi. *Assignments for Vibrational Specta of Benzene Derivatives*. Akadémiai Kiadó, Budapest (1973).